Iranian Journal of Science
https://doi.org/10.1007/s40995-024-01695-9

RESEARCH PAPER

A Robust Higher-Order Scheme for Fractional Delay Differential Equations Involving Caputo Derivative

Biswajit Prusty[1] · **Madhukant Sharma**[1]

Received: 23 January 2024 / Accepted: 28 July 2024

Abstract
This article considers nonlinear fractional delay differential equations involving Caputo's fractional derivative of order $\alpha \in (0, 1)$. We focus on designing a robust numerical algorithm of order $O(h^{4-\alpha})$. To achieve this, we developed a higher-order interpolation-based approximation for Caputo's derivative, which enables us to construct a robust numerical scheme for the considered problem. Furthermore, we discuss the stability and error analysis of the proposed higher-order scheme. Finally, numerous examples, including real-life applications, are evaluated to demonstrate the computational efficiency of the proposed algorithm.

Keywords Fractional differential equations · Delay differential equations · Interpolation · Error analysis

1 Introduction

The study of fractional differential equations (FDEs) has gained the intrinsic interest of researchers in recent decades. This is due to their recognition of analyzing various physical systems more efficiently than the classical models (Salahshour et al. 2015; Agarwal and Choi 2016; Diethelm and Ford 2010; Rivero et al. 2011; Chen et al. 2021). The literature contains numerous definitions of fractional derivatives and integrals, including those by Riemann-Liouville, Caputo, Grunwald-Letnikov, Caputo-Fabrizio, Atangana-Balaneu, and many more. A comprehensive study of these fractional derivatives was given by Samko et al. (1993), Jumarie (2009), Atangana and Secer (2013), and Atangana (2018) including their potential real-life applications, differing qualities, and their benefits and drawbacks. The Caputo's derivative gained considerable attention in the fractional calculus. The nonlocal property of Caputo's derivative and its applicability for analyzing intricate systems with memory effects are two primary reasons to consider it. It also allows the usage of initial and boundary conditions in the model governing equations. Furthermore, the derivative's order, say α, is a crucial control parameter that regulates the systems' trajectories' velocity. As a result, numerous authors considered Caputo's derivative to analyze real-world issues, such as the controller for a knee joint orthosis (Delavari and Jokar 2021), the dynamics of a second-grade fluid with Newtonian heating (Sene 2022), epidemics (Rehman et al. 2022), and the chaotic dynamics of the Jerk Fractional Model (Belhamiti et al. 2022). It is worth mentioning that the existence and controllability results of various types of FDEs have been investigated extensively (Dubey and Sharma 2014; Sharma 2021; Maes and Van 2023). A mild solution and an optimal pair of a nonlocal, non-autonomous fractional integrodifferential equation of Sobolev type have been established recently in (Sharma 2023). Further, the authors in (Haque et al. 2023) used the measure of non-compactness and fixed-point technique to derive sufficient criteria for the existence of solutions for an infinite system of Langevin FDEs.

On the other hand, difficulty in finding analytic solutions to FDEs motivated the researchers to develop considerable numerical algorithms for different FDEs (Rahimkhani and Ordokhani 2019; Yan et al. 2018; Kürkçüü et al. 2019; Zaky et al. 2020). Faheem et al. (2022) proposed a collocation method for solving a nonlinear coupled time-fractional diffusion system based on the Legendre wavelet using the Riemann-Liouville fractional integral operator.

✉ Madhukant Sharma
sharmamk003@gmail.com

[1] Dhirubhai Ambani Institute of Information and Communication Technology, Gandhinagar, Gujarat, India

Published online: 22 August 2024

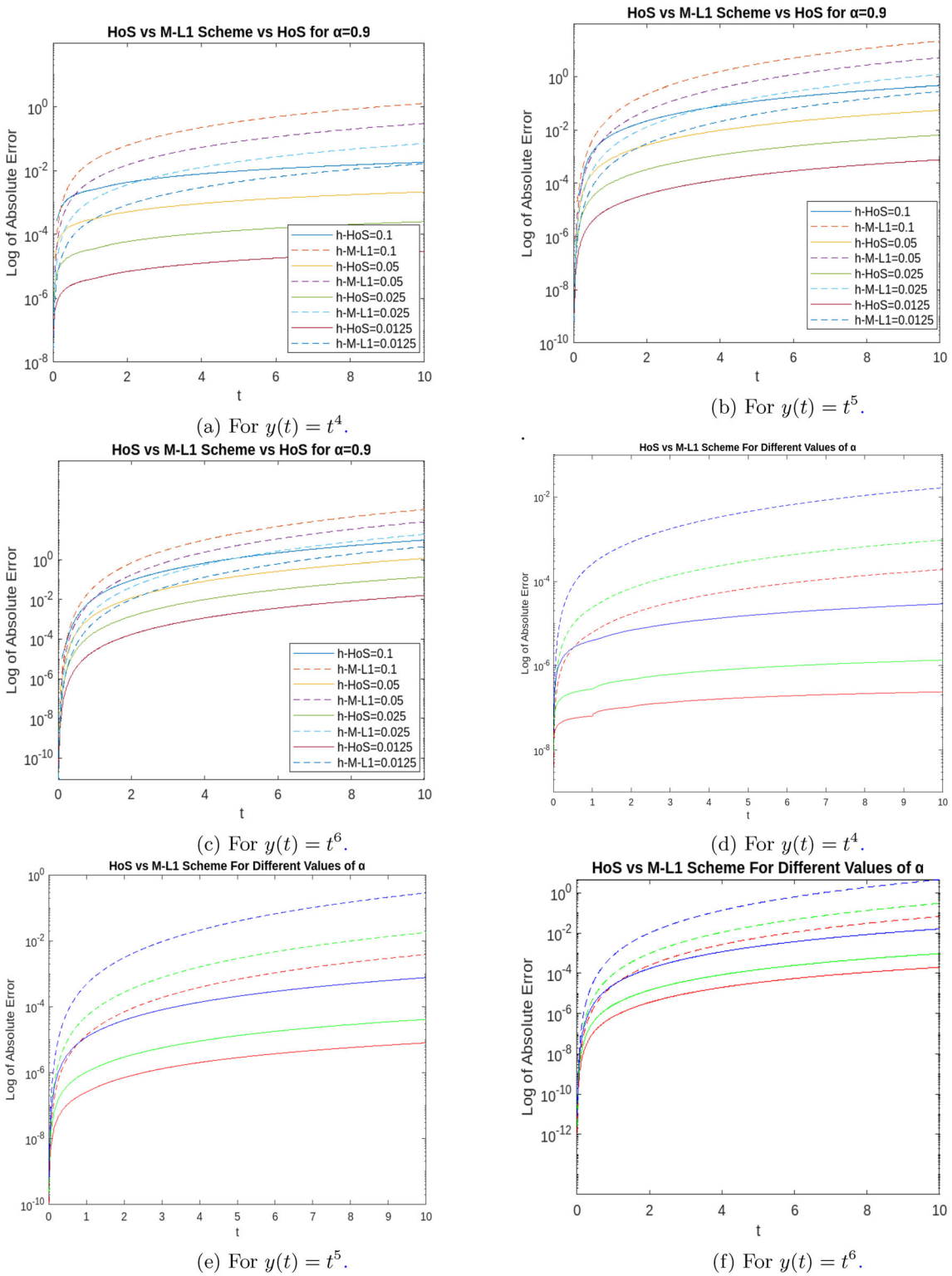

(a) For $y(t) = t^4$.

(b) For $y(t) = t^5$.

(c) For $y(t) = t^6$.

(d) For $y(t) = t^4$.

(e) For $y(t) = t^5$.

(f) For $y(t) = t^6$.

Fig. 1 Error plots for Example 5.1; solid-line is for HoS, dashed-line is for M-L1; red colour ($\alpha = 0.3$), green colour ($\alpha = 0.5$) and blue colour ($\alpha = 0.7$) in Fig. 1d–f

Agarwal et al. (2023) developed an efficient half-sweep type finite difference method for a one-dimensional fractional diffusion equation. Recently, Sabir and Rehman (2023) developed a numerical algorithm by combining Simpson's and Trapezoidal rule, which transformed the equivalent Volterra integral equation of FDE into a system

of algebraic equations. The authors also presented a detailed error analysis of the proposed scheme. Also, the authors of (Admon et al. 2023) used first-order optimization techniques, momentum method, and adaptive moment estimation method for designing deep feedforward neural network-based schemes to solve FDEs involving Caputo derivative. Several authors also adopted the Laplace transform residual power series (LTRPS) method to approximate solutions for numerous FDEs due to its high accuracy in solving fractional nonlinear equations and its easy calculation process (Alshammari et al. 2024; Khirsariya et al. 2024). For more details and other advanced procedures, please refer to the above and those listed.

Consider the following nonlinear fractional delay differential equation (FDDE):

$$\begin{cases} {}_0^C D_t^{\alpha} y(t) = G(t, y(t-\tau), y(t)) & \text{for } t \in I = [0, T],\ \alpha \in (0,1), \\ y(t) = \phi(t) & \text{for } t \in [-\tau, 0], \end{cases} \tag{1.1}$$

where τ be a positive real number, ${}_0^C D_t^{\alpha}$ denotes the Caputo derivative of order α with lower-limit 0, and $\phi \in C[-\tau, 0]$, a space of all continuous real-valued functions defined on $[-\tau, 0]$. The local and global existence results for the considered problem (1.1) can be found in (Lakshmikantham 2008). It is well-known that the solution of the considered nonlinear Eq. (1.1) can be approximated after linearizing it through Newton's Iterative Method. It is worth mentioning the following final linearized form of (1.1) in each of Newton's iterations: (for details, one may refer to Appendix A):

$$\begin{cases} {}_0^C D_t^{\alpha} y(t) = b(t) y(t) + g(t, y(t-\tau)) & \text{for } t \in I = [0, T],\ \alpha \in (0,1), \\ y(t) = \phi(t) & \text{for } t \in [-\tau, 0]. \end{cases} \tag{1.2}$$

It is evident that delays are ubiquitous in real-world systems and naturally occur in the governing differential equations of specific processes and physical systems that possess memory and heritage properties. Therefore, delay differential equations involving integer-order derivatives have received significant attention from researchers (Sriwastav et al. 2023; Sandoz et al. 2023; Elango 2023; Agiza et al. 2023; Pituk et al. 2023). However, the study of FDDEs is relatively recent and follows a similar growth trajectory in several areas. The results concerning the existence of solutions and stability analysis for several types of FDDEs can be found in (Deng et al. 2007; Liao and Ye 2009; Lazarević and Spasić 2009; Krol 2011; Morgado et al. 2013; Sharma and Dubey 2017). The computational complexities deriving the analytic solution of FDDEs have imperatively inclined researchers to design numerical algorithms for approximating their solutions (Jhinga and Daftardar-Gejji 2019; Raju and Madduri 2021; Behera and Ray 2022). In (Jhinga and Daftardar-Gejji 2019), the authors proposed a new predictor-corrector method of order $O(h^2)$ for solving FDDEs and discussed its error analysis in detail. Further, they also proved its efficacy for minimal values of the order of the fractional derivatives. Raju and Madduri et al. (2021) proposed two higher-order numerical methods of order $O(h^{3-\alpha})$ for approximating the solutions of FDDEs involving the Riemann-Liouville fractional derivative and the Caputo's fractional derivative, respectively. The authors employed interpolation-based and finite-difference methods for approximating the considered derivatives and presented a detailed stability and error analysis. Zaky et al. (2023) designed a $L1-$ approximation for the fractional derivative of variable order and developed a Galerkin spectral method for the spatial operator of second-order using Legendre polynomials. They also established the convergence and stability results for the proposed algorithm using discrete energy estimates. Using the fractional integral operational matrix based on Euler wavelets, Behera and Ray (2022) proposed a new numerical scheme for the fractional order pantograph Volterra delay integro-differential equation and discussed its convergence and error analysis. The study of stability analysis for multi-term FDDEs was performed recently by Yang et al. (2023), where the authors derived a region embedding technique and combined the same with the Laplace transform method and decoupling technique.

The references mentioned above and the lack of computationally efficient numerical schemes motivated us to design a robust higher-order method, i.e., of order $O(h^{4-\alpha})$, for approximating the solution of FDDE (1.2). First, in Sect. 2, we derived the interpolation-based approximation of the Caputo fractional derivative. Then, we incorporated it carefully in the equation (1.2), which resulted in a numerical scheme of order $O(h^{4-\alpha})$. Then, we established the stability results in Sect. 3 and discussed detailed error analysis in Sect. 4 for the proposed numerical algorithm. We considered examples of different FDDEs in Sect. 5 and demonstrated the computational efficiency of the proposed algorithm. Further, we compared the obtained results with the M-L1 scheme (Raju and Madduri 2021) and gave concluding remarks in Sect. 6. All the computations presented in this work have been performed over the Matlab online platform (MathWorks) version R2022.

2 Higher-Order Scheme(HoS)

This section presents a higher-order numerical scheme for the Eq. (1.2). To begin with, let us first introduce the definition of the Caputo fractional derivative.

Definition 2.1 (Caputo Fractional derivative (Diethelm and Ford 2010)) Let $\alpha \in (0,1]$. The operator ${}_0^C D_t^\alpha$ defined below is called the Caputo's derivative of order α with lower-limit 0:

$$ {}_0^C D_t^\alpha f(t) := \frac{1}{\Gamma(1-\alpha)} \int_0^t (t-s)^{-\alpha} f'(s) ds, $$

where f is continuously differentiable function on $[0, T]$.

Let us consider a partition $0 = t_0 < t_1 < t_2 < \ldots < t_l = lh = k\tau = T$ of I with fixed $l \in \mathbb{N}$, and uniform-spaced step size h. Now, at every point t_r, $r = 1, 2, \ldots, l$, the Eq. (1.2) can be written as,

$$ {}_0^C D_t^\alpha y(t_r) = g(t_r, y(t_r - \tau)) + b(t_r) y(t_r) = \zeta_{k\tau}(t_r) + b(t_r) y(t_r), \tag{2.1} $$

where the function $\zeta_{k\tau}$ is defined as in the Eq. (A.2). It is easy to derive the following:

$$ \begin{aligned} {}_0^C D_t^\alpha y(t_r) &= \frac{1}{\Gamma(1-\alpha)} \int_0^{t_r} (t_r - s)^{-\alpha} y'(s) ds \\ &= \frac{1}{\Gamma(1-\alpha)} \sum_{j=1}^{r} \int_{t_{j-1}}^{t_j} (t_r - s)^{-\alpha} y'(s) ds. \end{aligned} \tag{2.2} $$

Using Newton's Divided difference method, first we approximate y by a cubic polynomial at $t = t_{j-3}, t_{j-2}, t_{j-1}, t_j$, which will be given by:

$$ \begin{aligned} y(t) =& y(t_{j-3}) + (t - t_{j-3}) \left(\frac{y(t_{j-2}) - y(t_{j-3})}{h} \right) \\ &+ (t - t_{j-3})(t - t_{j-2}) \left(\frac{y(t_{j-3}) - 2y(t_{j-2}) + y(t_{j-1})}{2h^2} \right) \\ &+ \left((t - t_{j-3})(t - t_{j-2})(t - t_{j-1}) \right) y \\ &\left(\frac{y(t_{j-3}) - 3y(t_{j-2}) + 3y(t_{j-1}) - y(t_j)}{6h^3} \right) \\ &+ R_{1,j}(t), \end{aligned} \tag{2.3} $$

where $R_{1,j}(t) = \frac{y^{(4)}(\xi_j)}{4!} \prod_{i=j-3}^{j} (t - t_i)$, $\xi_j \in [t_{j-3}, t_j]$. On differentiating above, we get

$$ \begin{aligned} y'(t) =& \left(\frac{y(t_{j-2}) - y(t_{j-3})}{h} \right) \\ &+ (2t - t_{j-3} - t_{j-2}) \left(\frac{y(t_{j-3}) - 2y(t_{j-2}) + y(t_{j-1})}{2h^2} \right) \\ &+ \Big((t - t_{j-3})(t - t_{j-2}) + (t - t_{j-1})(t - t_{j-3}) \\ &+ (t - t_{j-2})(t - t_{j-1}) \Big) \left(\frac{y(t_{j-3}) - 3y(t_{j-2}) + 3y(t_{j-1}) - y(t_j)}{6h^3} \right) \\ &+ R'_{1,j}(t). \end{aligned} $$

This further implies the following:

$$ \begin{aligned} {}_0^C D_t^\alpha y(t_r) =& \sum_{j=1}^{r} \Big[c_{r-j}(y(t_{j-2}) - y(t_{j-3})) + m_{r-j}(y(t_{j-3}) - 2y(t_{j-2}) \\ &- y(t_{j-1})) + n_{r-j}(-y(t_{j-3}) + 3y(t_{j-2}) - 3y(t_{j-1}) + y(t_j)) \Big] \\ &+ R_2, \end{aligned} \tag{2.4} $$

where the constants c_j, m_j and n_j for $j = 0, 1, 2 \ldots, r-1$, and the truncation error R_2 are defined as follows:

$$ \begin{cases} c_j = \dfrac{h^{-\alpha}}{\Gamma(1-\alpha)} d_j^{1-\alpha}, \\ m_j = \dfrac{h^{-\alpha}}{\Gamma(1-\alpha)} \left[\left(j + \dfrac{5}{2} \right) d_j^{1-\alpha} - d_j^{2-\alpha} \right], \\ n_j = \dfrac{h^{-\alpha}}{\Gamma(1-\alpha)} \left[\dfrac{d_j^{3-\alpha}}{2} - (2+j) d_j^{2-\alpha} + \dfrac{d_j^{1-\alpha}}{6} (2(2+j)^2 + (3+j)(1+j)) \right], \\ R_2 = \displaystyle\sum_{j=1}^{r} \frac{R_{2j}}{\Gamma(1-\alpha)}, \text{ with } R_{2,j} = \int_{t_{j-1}}^{t_j} (t_r - s)^{-\alpha} R'_{1,j}(s) ds, \\ d_j^\beta = \dfrac{(j+1)^\beta - j^\beta}{\beta}, \; j = 0, 1, 2, \ldots, r-1 \text{ and } \beta > 0. \end{cases} \tag{2.5} $$

Using (2.4) in (2.1), then, for $r = 1$, we get the following:

$$ \begin{aligned} (n_0 - b(t_1)) y(t_1) =& (c_0 - m_0 + n_0) \phi(t_{-2}) \\ &+ (2m_0 - c_0 - 3n_0) \phi(t_{-1}) \\ &+ (3n_0 - m_0) \phi(t_0) \\ &+ \zeta_{k\tau}(t_1) - R_2. \end{aligned} \tag{2.6} $$

Similarly for $r = 2$, we have

$$ \begin{aligned} (n_0 - b(t_2)) y(t_2) =& (c_1 - m_1 + n_1) \phi(t_{-2}) + (2m_1 - c_1 - 3n_1 \\ &+ c_0 - m_0 + n_0) \phi(t_{-1}) + (3n_1 - m_1 - c_0 \\ &+ 2m_0 - 3n_0) \phi(t_0) \\ &+ (3n_0 - m_0 + n_1) y(t_1) \\ &+ \zeta_{k\tau}(t_2) - R_2. \end{aligned} \tag{2.7} $$

Also, for $r = 3, 4, \ldots, l$, we derive the following scheme

$$
\begin{aligned}
(n_0 - b(t_r))y(t_r) = \sum_{j=1}^{r-3} \Big[& - n_{r-j} \\
& - m_{r-j-1} + 3n_{r-j-1} - c_{r-j-2} + 2m_{r-j-2} \\
& - 2n_{r-j-2} + c_{r-j-3} - m_{r-j-3} + n_{r-j-3} \Big] y(t_j) \\
& + (-n_2 - m_1 + 3n_1 - c_0 \\
& + 2m_0 - 3n_0) y(t_{r-2}) \\
& + (-n_1 + 3n_0 - m_0) y(t_{r-1}) \\
& + (c_{r-1} - m_{r-1} + n_{r-1}) \phi(t_{-2}) \\
& + (-c_{r-1} + 2m_{r-1} - 3n_{r-1} \\
& + c_{r-2} - m_{r-2} + n_{r-2}) \phi(t_{-1}) \\
& + (-m_{r-1} + 3n_{r-1} - c_{r-2} + 2m_{r-2} \\
& - 3n_{r-2} + c_{r-3} - m_{r-3} + n_{r-3}) \phi(t_0) \\
& + \zeta_{k\tau}(t_r) - R_2.
\end{aligned} \tag{2.8}
$$

We denote $y_r \approx y(t_r)$, $b_r = b(t_r)$, $\zeta_{k\tau}^r \approx \zeta_{k\tau}(t_r)$ for $r = 1, 2, ..., l$, respectively. Then, we have the following numerical scheme for the solution of (1.2):

$$
\begin{aligned}
(n_0 - b_1)y_1 = & (c_0 - m_0 + n_0)\phi(t_{-2}) + (2m_0 - c_0 \\
& - 3n_0)\phi(t_{-1}) + (3n_0 - m_0)\phi(t_0) + \zeta_{k\tau}^1,
\end{aligned} \tag{2.9}
$$

$$
\begin{aligned}
(n_0 - b_2)y_2 = & (c_1 - m_1 + n_1)\phi(t_{-2}) + (2m_1 - c_1 \\
& - 3n_1 + c_0 - m_0 + n_0)\phi(t_{-1}) + (3n_1 - m_1 - c_0 \\
& + 2m_0 - 3n_0)\phi(t_0) + (3n_0 - m_0 + n_1)y(t_1) + \zeta_{k\tau}^2,
\end{aligned} \tag{2.10}
$$

$$
\begin{aligned}
(n_0 - b_r)y_r = \sum_{j=1}^{r-3} \Big[& - n_{r-j} - m_{r-j-1} \\
& + 3n_{r-j-1} - c_{r-j-2} + 2m_{r-j-2} - 2n_{r-j-2} + c_{r-j-3} - m_{r-j-3} \\
& + n_{r-j-3} \Big] y_j + (-n_2 - m_1 + 3n_1 - c_0 \\
& + 2m_0 - 3n_0) y_{r-2} + (-n_1 + 3n_0 - m_0) y_{r-1} \\
& + (c_{r-1} - m_{r-1} + n_{r-1})\phi(t_{-2}) + (-c_{r-1} + 2m_{r-1} \\
& - 3n_{r-1} + c_{r-2} - m_{r-2} + n_{r-2})\phi(t_{-1}) \\
& + (-m_{r-1} + 3n_{r-1} - c_{r-2} + 2m_{r-2} - 3n_{r-2} + c_{r-3} \\
& - m_{r-3} + n_{r-3})\phi(t_0) + \zeta_{k\tau}^r, \quad \text{for} \quad r = 3, 4, ..., l.
\end{aligned} \tag{2.11}
$$

3 Stability

Theorem 3.1 *Let $b \leq -1$, and let y_r, x_r, $r = 1, 2, 3, ..., l$, be the approximate solution and perturbed solution, respectively, obtained from the numerical scheme and that of,*

$$
\begin{aligned}
(n_0 - b_1)x_1 = & (c_0 - m_0 + n_0)\tilde{\phi}(t_{-2}) + (2m_0 - c_0 \\
& - 3n_0)\tilde{\phi}(t_{-1}) + (3n_0 - m_0)\tilde{\phi}(t_0) + \tilde{\zeta}_{k\tau}^1 - R_2, \\
(n_0 - b_2)x_2 = & (c_1 - m_1 + n_1)\tilde{\phi}(t_{-2}) \\
& + (2m_1 - c_1 - 3n_1 + c_0 - m_0 + n_0)\tilde{\phi}(t_{-1}) \\
& + (3n_1 - m_1 + 2m_0 - c_0 - 3n_0)\tilde{\phi}(t_0) \\
& + (3n_0 - m_0 - n_1)x_1 + \tilde{\zeta}_{k\tau}^2 - R_2, \\
(n_0 - b_r)x_r = & \sum_{j=1}^{r-3} (-n_{r-j} - m_{r-j-1} + 3n_{r-j-1} \\
& - c_{r-j-2} + 2m_{r-j-2} - 2n_{r-j-2} + c_{r-j-3} - m_{r-j-3} \\
& + n_{r-j-3})x_j + (c_{r-1} - m_{r-1} + n_{r-1})\tilde{\phi}(t_{-2}) \\
& + (-n_2 - m_1 + 3n_1 - c_0 + 2m_0 - 3n_0)x_{r-2} \\
& + (-n_1 + 3n_0 - m_0)x_{r-1} + (-c_{r-1} + 2m_{r-1} \\
& - 3n_{r-1} + c_{r-2} - m_{r-2} + n_{r-2})\tilde{\phi}(t_{-1}) \\
& + (-m_{r-1} + 3n_{r-1} - c_{r-2} + 2m_{r-2} - 3n_{r-2} \\
& + c_{r-3} - m_{r-3} + n_{r-3})\tilde{\phi}(t_0) \\
& + \tilde{\zeta}_{k\tau}^r - R_2, \quad \text{for} \quad r = 3, 4, ..., l,
\end{aligned}
$$

where $\tilde{\phi}$ be a continuous real-valued function defined on $[-\tau, 0]$ such that

$$
\max_{-\tau \leq t \leq 0} (\phi(t) - \tilde{\phi}(t)) \leq \epsilon \text{ and } \max_{0 \leq t \leq T} (\zeta_{k\tau}(t) - \tilde{\zeta}_{k\tau}(t)) \leq \tilde{\epsilon}. \tag{3.1}
$$

If we define $\epsilon_r = y_r - x_r$ for $r = 1, 2, ..., l$, then,

$$|\epsilon_r| \leq \epsilon + 3.5\tilde{\epsilon}.$$

Proof We use the principle of mathematical induction to establish our claim. For the case $r = 1$, using the definitions of x_1, y_1, ϵ_1, we deduce the following:

$$
\begin{aligned}
(n_0 - b_1)\epsilon_1 = & (c_0 - m_0 + n_0)(\phi(t_{-2}) - \tilde{\phi}(t_{-2})) \\
& + (2m_0 - c_0 - 3n_0)(\phi(t_{-1}) - \tilde{\phi}(t_{-1})) \\
& + (3n_0 - m_0)(\phi(t_0) - \tilde{\phi}(t_0)) + \zeta_{k\tau}^1 - \tilde{\zeta}_{k\tau}^1.
\end{aligned}
$$

On taking absolute values and using the inequality (3.1), we get

$$
\begin{aligned}
& (n_0 - b_1)|\epsilon_1| \leq n_0\epsilon + \tilde{\epsilon} \Rightarrow |\epsilon_1| \leq (n_0\epsilon + \tilde{\epsilon})/(n_0 - b_1) \\
& \leq (n_0\epsilon + \tilde{\epsilon})/n_0 \leq \epsilon + \tilde{\epsilon}/n_0 \leq \epsilon + 3.5\tilde{\epsilon}.
\end{aligned}
$$

Again, for the case $r = 2$, using the definitions of x_2, y_2, ϵ_2, we deduce the following:

$$\begin{aligned}(n_0-b_2)\epsilon_2 =&(c_1-m_1+n_1)(\phi(t_{-2}-\tilde{\phi}(t_{-2}))\\&+(2m_1-c_1-3n_1+c_0-m_0+n_0)(\phi(t_{-1}-\tilde{\phi}(t_{-1}))\\&+(3n_1-m_1+2m_0-c_0-3n_0)(\phi(t_0)-\tilde{\phi}(t_0))\\&+(3n_0-m_0-n_1)\epsilon_1+\zeta_{k\tau}^2-\tilde{\zeta}_{k\tau}^2.\end{aligned}$$

Further, on taking absolute values and using the inequality (3.1), we get

$$\begin{aligned}(n_0-b_2)|\epsilon_2| \le& |n_1+m_0-2n_0|\epsilon\\&+|3n_0-m_0-n_1||\epsilon+\tilde{\epsilon}/n_0|+\tilde{\epsilon}\\ \le& (|n_1+m_0-2n_0|+|3n_0-m_0-n_1|)\epsilon\\&+\left(1+\frac{|3n_0-m_0-n_1|}{n_0}\right)\tilde{\epsilon},\end{aligned}$$

which implies the following

$$|\epsilon_2| \le \epsilon+\left(\frac{1}{n_0-b_2}\right)\left(1+\frac{|3n_0-m_0-n_1|}{n_0}\right)\tilde{\epsilon} \le \epsilon+3.5\tilde{\epsilon}.$$

Similarly, for the case $r=3$, using the definitions of x_3, y_3, ϵ_3, we deduce the following:

$$\begin{aligned}(n_0-b_3)\epsilon_3 =&(-n_2-m_1+3n_1-c_0+2m_0-3n_0)\epsilon_1\\&+(-n_1+3n_0-m_0)\epsilon_2+(c_2-m_2+n_2)\epsilon\\&+(-c_2+2m_2-3n_2+c_1-m_1+n_1)\epsilon+(-m_2\\&+3n_2-c_1+2m_1-3n_1+c_0-m_0+n_0)\epsilon+\tilde{\epsilon}.\end{aligned}$$

Using the inequality (3.1) and taking absolute values, we get

$$\begin{aligned}(n_0-b_3)|\epsilon_3| \le& \Big(\Big|n_2+m_1-2n_1+c_0-m_0\\&+n_0\Big|+\Big|-n_2-m_1+3n_1-c_0\\&+2m_0-3n_0\Big|+\Big|-n_1+3n_0\\&-m_0\Big|\Big)\epsilon+\Big(1+\Big|-n_2-m_1+3n_1-c_0\\&+2m_0-3n_0\Big|+\Big|-n_1+3n_0-m_0\Big|\Big)3.5\tilde{\epsilon},\end{aligned}$$

which also implies the following

$$(n_0-b_3)|\epsilon_3| \le n_0\epsilon+(1+n_0)3.5\tilde{\epsilon} \Rightarrow |\epsilon_3| \le \epsilon+3.5\tilde{\epsilon}.$$

Let us assume that $|\epsilon_i| \le \epsilon+3.5\tilde{\epsilon}$ for $i \le r$. We will show that the result holds true for $i=r+1$, i.e.,

$$|\epsilon_{r+1}| \le \epsilon+3.5\tilde{\epsilon}.$$

Using the inequality (3.1), the definitions of $x_{r+1}, y_{r+1}, \epsilon_{r+1}$, and taking absolute values, we get

$$\begin{aligned}(n_0-b_{r+1})|\epsilon_{r+1}| \le& \sum_{j=1}^{r-2}\Big|-n_{r-j+1}-m_{r-j}+3n_{r-j}-c_{r-j-2}\\&+2m_{r-j-1}-3n_{r-j-1}+c_{r-j-2}\\&-m_{r-j-2}+n_{r-j-2}\Big|\Big|\epsilon_j\Big|+\Big|-n_2-m_1\\&+3n_1-c_0+2m_0-3n_0\Big|\Big|\epsilon_{r-1}\Big|\\&+\Big|-n_1+3n_0-m_0\Big|\Big|\epsilon_r\Big|+\Big|c_r\\&-m_r+n_r-c_r+2m_r-3n_r+c_{r-1}-m_{r-1}\\&+n_{r-1}-m_r+3n_r-c_{r-1}+2m_{r-1}\\&-3n_{r-1}+c_{r-2}-m_{r-2}+n_{r-2}\Big|\epsilon+\tilde{\epsilon}.\end{aligned}$$

Further, we use the assumption that $|\epsilon_i| \le \epsilon+3.5\tilde{\epsilon}$ for $i \le r$. Then, we get

$$\begin{aligned}(n_0-b_{r+1})|\epsilon_{r+1}| \le& n_0\epsilon+\Big(1+\Big|-n_2-m_1+3n_1-c_0\\&+2m_0-3n_0\Big|+\Big|-n_1+3n_0-m_0\Big|+\Big|-n_r\\&-m_{r-1}+2n_{r-1}-c_{r-2}+m_{r-2}-n_{r-2}+n_2\\&+m_1-2n_1+c_0-m_0+n_0\Big|\Big)3.5\tilde{\epsilon}\\ \le& n_0\epsilon+(1+n_0)3.5\tilde{\epsilon} \Rightarrow |\epsilon_{r+1}| \le \epsilon+3.5\tilde{\epsilon}.\end{aligned}$$

This establishes our claim.

□

4 Error Analysis

Theorem 4.1 *Suppose* $y \in C^4[0,T]$ *and let* y_r, $r=1,2,...,l$, *be the approximate solution derived from numerical algorithm* (2.9)–(2.11) *for the FDDE* (1.2). *Then* (*for the interval* $0 \le t_i \le j\tau$ *for* $i=1,...,r$)

$$|y_r-y(t_r)| \le Nh^{4-\alpha} \quad \text{for } r=3,4,...,l. \tag{4.1}$$

Proof First we define $e_r=y_r-y(t_r)$ for $r=1,2,...,l$. On subtracting the Eqs. (2.6)–(2.8) from the Eqs. (2.9)–(2.11), respectively, we get

$$(n_0-b_1)e_1=(\zeta_{k\tau}^1-\zeta_{k\tau}(t_1))-R_2, \tag{4.2}$$

$$(n_0-b_2)e_2=(3n_0-m_0+n_1)e_1+(\zeta_{k\tau}^2-\zeta_{k\tau}(t_2))-R_2, \tag{4.3}$$

$$
\begin{aligned}
(n_0 - b_r)e_r = \sum_{j=1}^{r-3} \Big[& - n_{r-j} - m_{r-j-1} \\
& + 3n_{r-j-1} - c_{r-j-2} + 2m_{r-j-2} \\
& - 2n_{r-j-2} + c_{r-j-3} - m_{r-j-3} \\
& + n_{r-j-3} \Big] e_j + (-n_2 - m_1 \\
& + 3n_1 - c_0 + 2m_0 - 3n_0)e_{r-2} \\
& + (-n_1 + 3n_0 - m_0)e_{r-1} \\
& + (\zeta_{k\tau}^2 - \zeta_{k\tau}(t_2)) - R_2, \quad \text{for} \quad r = 3, 4, ..., l.
\end{aligned} \tag{4.4}
$$

First, we establish (4.1) for the case $r = 1$. For the same, we take absolute values on both sides and use the Lemma A.3, which yields the following result from (4.2):

$$
\begin{aligned}
|e_1| &\le \frac{|\zeta_{k\tau}^1 - \zeta_{k\tau}(t_1)| + |R_2|}{n_0 - b_1} \\
&\le \left(\frac{1}{n_0 - b_1}\right) \left[\sum_{i=1}^{j-1} \left(\frac{7}{2}\right)^i + 1 \right] Mh^{4-\alpha} \le Nh^{4-\alpha}.
\end{aligned}
$$

Secondly, we establish (4.1) for the case $r = 2$. Again, we take absolute values on both sides of (4.3) and use the Lemma A.3 along with the above inequality. This yields the following result:

$$
\begin{aligned}
|e_2| &\le \left(\frac{1}{n_0 - b_2}\right) \Big| (3n_0 - m_0 - n_1)e_1 + (\zeta_{k\tau}^2 - \zeta_{k\tau}(t_2)) - R_2 \Big| \\
&\le \frac{|3n_0 - m_0 - n_1|}{n_0} |e_1| + |\zeta_{k\tau}^2 - \zeta_{k\tau}(t_2)| + |R_2| \\
&\le \frac{5}{2}|e_1| + \left[\sum_{i=1}^{j-1} \left(\frac{7}{2}\right)^i + 1 \right] Mh^{4-\alpha} \\
&\le \frac{7}{2} \left[\sum_{i=1}^{j-1} \left(\frac{7}{2}\right)^i + 1 \right] Mh^{4-\alpha} = \left[\sum_{i=1}^{j} \left(\frac{7}{2}\right)^i \right] Mh^{4-\alpha} \le Nh^{4-\alpha}.
\end{aligned}
$$

Next, we establish (4.1) for the case $r = 3$. Again, we take absolute values on both sides on (4.4) and use the Lemma A.3 along with the above inequalities for the cases $r = 1$ and $r = 2$. We get

$$
\begin{aligned}
|e_3| &\le \left(\frac{1}{n_0 - b_3}\right) \Big[| - n_2 - m_1 + 3n_1 - c_0 + 2m_0 - 3n_0||e_1| \\
&\quad + | - n_1 + 3n_0 - m_0||e_2| + |\zeta_{k\tau}^3 - \zeta_{k\tau}(t_3)| + |R_2| \Big] \\
&\le \left(\frac{1}{n_0 - b_3}\right) \Big[| - n_2 - m_1 + 2n_1 - c_0 + m_0| Nh^{4-\alpha} + Nh^{4-\alpha} \Big] \\
&\le \left(\frac{1 + n_0}{n_0 - b_3}\right) Nh^{4-\alpha} \le Nh^{4-\alpha}.
\end{aligned}
$$

Now, we apply the strong principle of the mathematical induction hypothesis to establish the result for $i = 1, 2, ..., r$. For the same, we assume that the result holds for the case $i \le r - 1$, i.e.,

$$
|e_i| \le Nh^{4-\alpha}, \qquad \text{for } i \le r - 1.
$$

We establish that $|e_r| \le Nh^{4-\alpha}$. Using the above inequality in the Eq. (4.4), we get

$$
\begin{aligned}
|e_r| &\le \left(\frac{1}{n_0 - b_r}\right) \Big[\sum_{j=1}^{r-3} | - n_{r-j} - m_{r-j-1} + 3n_{r-j-1} - c_{r-j-1} + | \\
&\quad + 2m_{r-j-2} - 2n_{r-j-2} + c_{r-j-3} - m_{r-j-3} + n_{r-j-3}||e_j|| \\
&\quad - n_2 - m_1 + 3n_1 - c_0 + 2m_0 - 3n_0||e_{r-2}| + | \\
&\quad - n_1 + 3n_0 - m_0||e_r| + |\zeta_{k\tau}^r - \zeta_{k\tau}(t_r)| + |R_2| \Big] \\
&\le \left(\frac{1}{n_0 - b_r}\right) \Big[\Big(| - n_2 - m_1 + 3n_1 - c_0 + 2m_0 - 3n_0| + | - n_1 \\
&\quad + 3n_0 - m_0| + | - n_r - m_{r-1} + 2n_{r-1} - c_{r-2} \\
&\quad + m_{r-2} - n_{r-2} + n_2 + m_1 - 2n_1 + c_0 \\
&\quad - m_0 + n_0| + 1 \Big) Nh^{4-\alpha} \Big] \\
&\le \left(\frac{1}{n_0 - b_r}\right) \Big[\Big| - n_r - m_{r-1} + 2n_{r-1} - c_{r-2} + m_{r-2} \\
&\quad - n_{r-2} + n_0 \Big| + 1 \Big] Nh^{4-\alpha} \\
&\le \left(\frac{1 + n_0}{n_0 - b_r}\right) Nh^{4-\alpha} \le Nh^{4-\alpha}.
\end{aligned}
$$

Hence, (4.1) be proved. □

5 Applications and Illustrations

This section demonstrates the computational efficiency of the HoS for approximating the solutions of FDDEs. We consider six examples in this section with varieties of possible exact solutions based on the initial delay functions. For instance, we consider three cases and approximate solutions using HoS in the first two examples. Next, we consider fully nonlinear FDDE in Example 5.3 with two instances and approximate its solution after carefully applying Newton's iterative method. Thereafter, we apply the proposed HoS scheme for a FDDE in Example 5.4 whose exact solution is not polynomial. The last two examples are real-life applications to analyze chaotic behavior and the stability of solutions.

Example 5.1 Consider the following FDDE

$$
{}_0^C D_t^\alpha y(t) + y(t) = y(t-1) + g(t) \quad \text{for } t \in [0, 10], \tag{5.1}
$$

where g be the real-valued function such that $y(t) = t^i$, for $i = 4, 5, 6$, be the exact solution of (5.1) with the delay functions $\phi(t) = t^i$, for $i = 4, 5, 6$, defined on $[-1, 0]$, respectively.

Table 1 Errors for $\alpha = 0.3$ and $\alpha = 0.5$ in Example 5.1 for $y(t) = t^4$

h	HoS ($\alpha = 0.3$)		M-L1 scheme ($\alpha = 0.3$)		HoS ($\alpha = 0.5$)		M-L1 scheme ($\alpha = 0.5$)	
	L_∞ error	EOC	L_∞ error	EOC	L_∞ error	EOC	L_∞ error	EOC
0.1	4.97×10^{-4}	–	4.87×10^{-2}	–	1.90×10^{-3}	–	1.66×10^{-1}	–
0.05	3.91×10^{-5}	3.67	4.87×10^{-2}	2.64	1.71×10^{-4}	3.49	2.98×10^{-2}	2.47
0.025	3.06×10^{-6}	3.67	1.20×10^{-3}	2.70	1.52×10^{-5}	3.49	5.30×10^{-3}	2.49
0.0125	2.39×10^{-7}	3.68	1.92×10^{-4}	2.64	1.35×10^{-6}	3.49	9.49×10^{-4}	2.48

Table 2 Errors for $\alpha = 0.3$ and $\alpha = 0.5$ in Example 5.1 for $y(t) = t^5$

h	HoS (α=0.3)		M-L1 scheme ($\alpha = 0.3$)		HoS (α=0.5)		M-L1 scheme (α=0.5)	
	L_∞ error	EOC	L_∞ error	EOC	L_∞ error	EOC	L_∞ error	EOC
0.1	1.64×10^{-2}	–	9.61×10^{-1}	–	5.73×10^{-2}	–	3.10	–
0.05	1.30×10^{-3}	3.65	1.54×10^{-1}	2.64	5.20×10^{-3}	3.46	5.60×10^{-1}	2.46
0.025	1.03×10^{-4}	3.65	2.40×10^{-2}	2.68	4.63×10^{-4}	3.48	1.00×10^{-1}	2.47
0.0125	8.12×10^{-6}	3.66	3.90×10^{-3}	2.62	4.12×10^{-5}	3.49	1.80×10^{-2}	2.48

Table 3 Errors for $\alpha = 0.3$ and $\alpha = 0.5$ in Example 5.1 for $y(t) = t^6$

h	HoS (α=0.3)		M-L1 scheme ($\alpha = 0.3$)		HoS (α=0.5)		M-L1 scheme (α=0.5)	
	L_∞ error	EOC	L_∞ error	EOC	L_∞ error	EOC	L_∞ error	EOC
0.1	3.87×10^{-1}	–	1.62×10^{1}	–	1.28	–	5.08×10^{1}	–
0.05	3.12×10^{-2}	3.62	2.62	2.62	1.16×10^{-1}	3.46	9.23	2.45
0.025	2.50×10^{-3}	3.62	4.18×10^{-1}	2.64	1.02×10^{-2}	3.46	1.66	2.47
0.0125	1.95×10^{-4}	3.66	6.61×10^{-2}	2.65	9.37×10^{-4}	3.47	2.97×10^{-1}	2.48

Table 4 Errors for $\alpha = 0.3$ and $\alpha = 0.5$ in Example 5.2 for $y(t) = t^4$

h	HoS (α=0.3)		M-L1 scheme ($\alpha = 0.3$)		HoS (α=0.5)		M-L1 scheme (α=0.5)	
	L_∞ error	EOC	L_∞ error	EOC	L_∞ error	EOC	L_∞ error	EOC
0.1	1.90×10^{-4}	–	2.33×10^{-2}	–	5.88×10^{-4}	–	7.19×10^{-2}	–
0.05	1.53×10^{-5}	3.63	3.70×10^{-3}	2.65	5.28×10^{-5}	3.47	1.29×10^{-2}	2.47
0.025	1.22×10^{-6}	3.65	5.85×10^{-4}	2.66	4.74×10^{-6}	3.47	2.30×10^{-3}	2.48
0.0125	9.59×10^{-8}	3.66	9.17×10^{-5}	2.67	4.23×10^{-7}	3.48	4.10×10^{-4}	2.48

Table 5 Errors for $\alpha = 0.3$ and $\alpha = 0.5$ in Example 5.2 for $y(t) = t^5$

h	HoS(α=0.3)		M-L1 scheme($\alpha = 0.3$)		HoS(α=0.5)		M-L1 scheme(α=0.5)	
	L_∞ error	EOC	L_∞ error	EOC	L_∞ error	EOC	L_∞ error	EOC
0.1	7.90×10^{-3}	-	5.33×10^{-1}	-	2.50×10^{-2}	-	1.63	-
0.05	6.26×10^{-4}	3.65	8.55×10^{-2}	2.64	2.20×10^{-3}	3.50	2.94×10^{-1}	2.46
0.025	4.93×10^{-5}	3.66	1.35×10^{-2}	2.66	2.00×10^{-4}	3.45	5.27×10^{-2}	2.48
0.0125	3.87×10^{-6}	3.67	2.10×10^{-0}	2.68	1.78×10^{-5}	3.49	9.40×10^{-3}	2.48

Table 6 Errors for $\alpha = 0.3$ and $\alpha = 0.5$ in Example 5.2 for $y(t) = t^6$

h	HoS(α=0.3)		M-L1 scheme($\alpha = 0.3$)		HoS(α=0.5)		M-L1 scheme(α=0.5)	
	L_∞ error	EOC	L_∞ error	EOC	L_∞ error	EOC	L_∞ error	EOC
0.1	2.15×10^{-1}	-	9.98	-	6.75×10^{-1}	-	3.02×10^{1}	-
0.05	1.73×10^{-2}	3.63	1.61	2.63	6.12×10^{-2}	3.46	5.48	2.46
0.025	1.40×10^{-3}	3.62	2.56×10^{-1}	2.65	5.50×10^{-3}	3.47	9.86×10^{-1}	2.47
0.0125	1.08×10^{-4}	3.69	4.05×10^{-2}	2.66	4.90×10^{-4}	3.48	1.76×10^{-1}	2.48

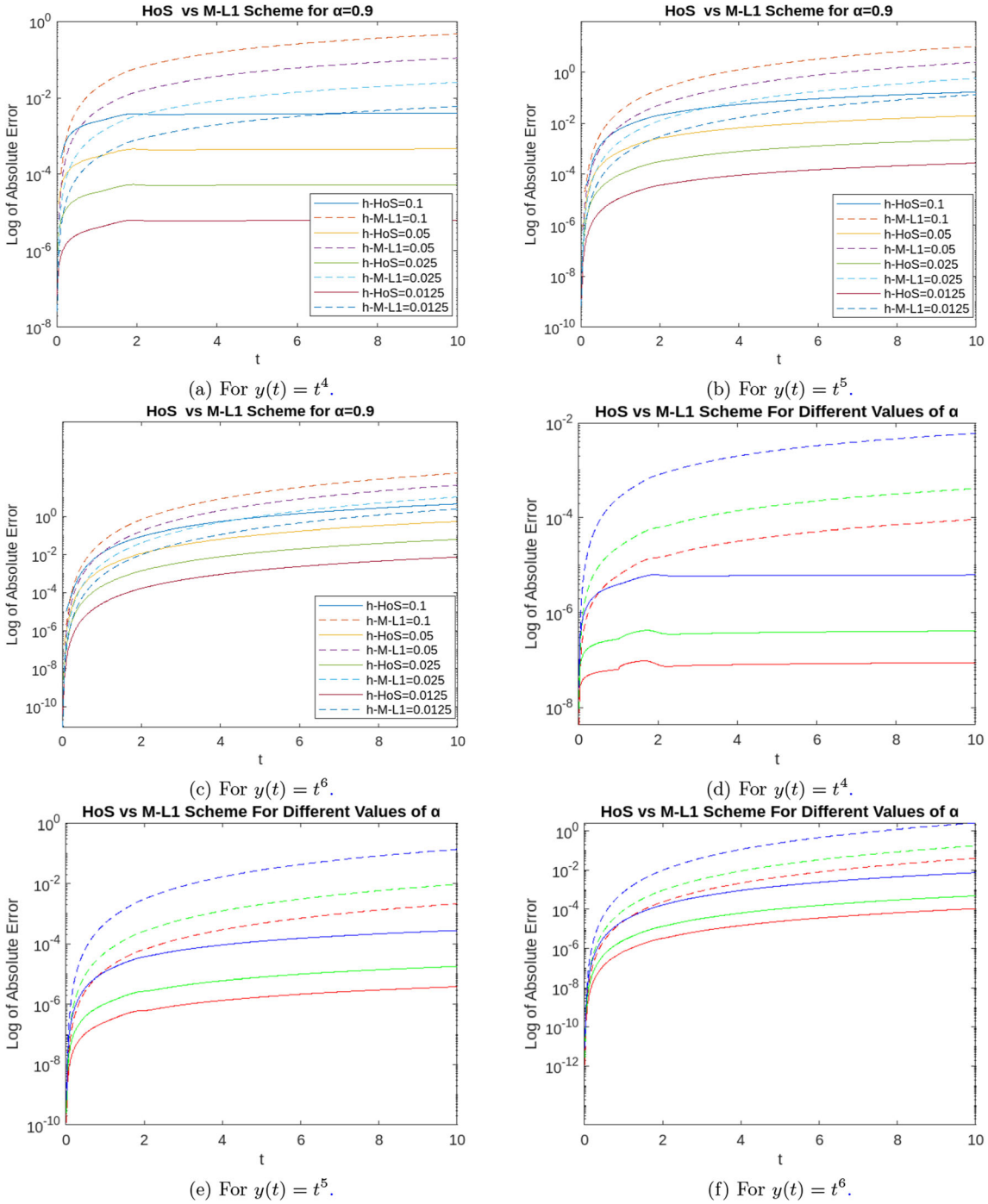

(a) For $y(t) = t^4$. (b) For $y(t) = t^5$.

(c) For $y(t) = t^6$. (d) For $y(t) = t^4$.

(e) For $y(t) = t^5$. (f) For $y(t) = t^6$.

Fig. 2 Error plots for Example 5.2; solid-line is for HoS, dashed-line is for M-L1; red colour ($\alpha = 0.3$), green colour ($\alpha = 0.5$) and blue colour ($\alpha = 0.7$) in Fig. 2d–f

Table 7 Errors for $\alpha = 0.9$ in Example 5.3 for $y(t) = t^4$

h	HoS			M-L1 scheme		
	L_∞ error	EOC	Time(s)	L_∞ error	EOC	Time(s)
0.1	4.50×10^{-3}	–	0.91	2.24×10^{-2}	–	0.32
0.05	5.58×10^{-4}	3.25	3.13	6.00×10^{-3}	1.91	1.03
0.025	6.65×10^{-5}	3.07	11.86	1.50×10^{-3}	2.01	3.87
0.0125	7.86×10^{-6}	3.08	32.07	4.00×10^{-4}	2.06	10.49
0.00625	9.22×10^{-7}	3.09	75.09	1.00×10^{-4}	2.68	24.36

Table 8 Errors for $\alpha = 0.9$ in Example 5.3 for $y(t) = t^5$

h	HoS			M-L1 scheme		
	L_∞ error	EOC	Time(s)	L_∞ error	EOC	Time(s)
0.1	7.90×10^{-3}	–	1.16	3.50×10^{-2}	–	0.38
0.05	1.10×10^{-3}	2.84	3.93	9.70×10^{-3}	1.87	1.32
0.025	1.40×10^{-4}	2.97	14.68	2.40×10^{-3}	1.99	4.77
0.0125	1.70×10^{-5}	3.04	39.45	5.80×10^{-4}	2.04	13.00
0.00625	2.02×10^{-6}	3.07	94.74	1.30×10^{-4}	2.07	30.60

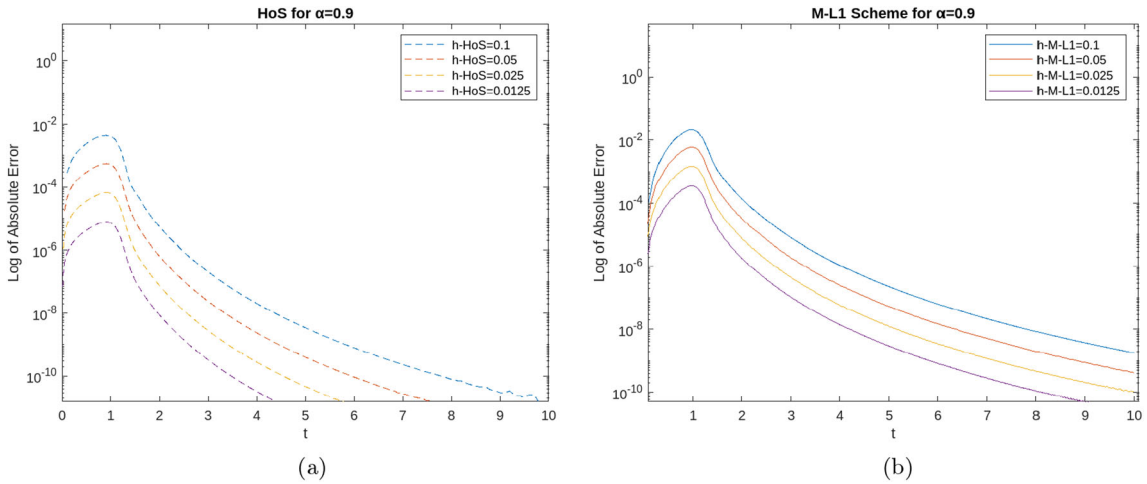

Fig. 3 Error plot of Example, for 5.3 for $y(t) = t^4$

Example 5.2 Consider the following nonlinear FDDE

$$ {}_0^C D_t^\alpha y(t) + y(t) = \frac{y(t-1)}{1 + y(t-1)^2} + g(t) \quad \text{for } t \in [0, 10], \tag{5.2} $$

where g be the real-valued function such that $y(t) = t^i$, $i = 4, 5, 6$, become the exact solution of the problem (5.2) with the delay function $\phi(t) = t^i$, for $i = 4, 5, 6$, defined on $[-1, 0]$, respectively.

Illustrations of Example 5.1 and5.2 First, we determined the functions g, for each $i = 4, 5, 6$, from Eqs. (5.1) and (5.2). For $\alpha = 0.3$ and $\alpha = 0.5$ with different step sizes, we applied our proposed scheme and compared the same with the M-L1 Scheme (Raju and Madduri 2021). For Example 5.1, the results are presented in Tables 1, 2, and 3 for the cases $i = 4, 5$, and 6, respectively. Similarly, the results for Example 5.2 are presented in Tables 4, 5, and 6 for each case $i = 4, 5$, and 6, respectively. It can be observed from the tables that the expected order of convergence (EOC) matches the theoretical results obtained in Theorem 4.1 and the $L_\infty-$error decreases whenever the step size h decreases.

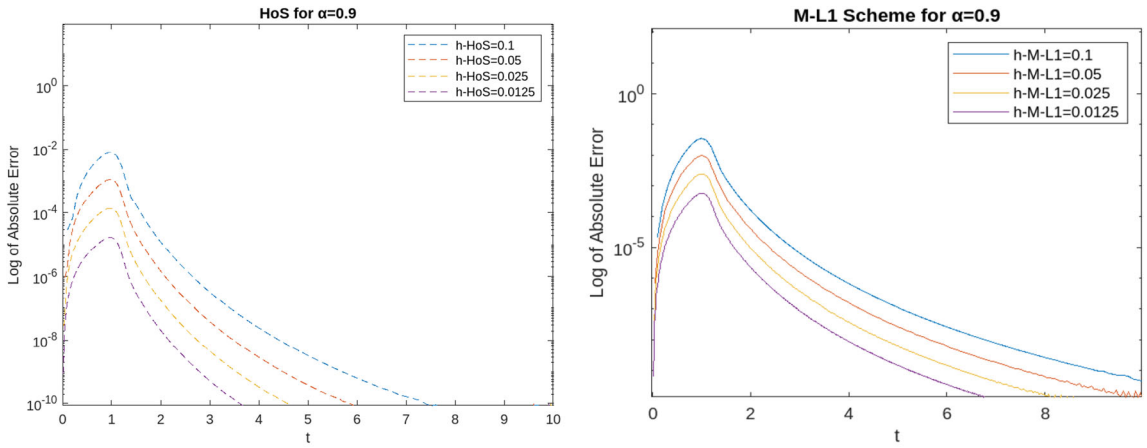

Fig. 4 Error plot of Example 5.3 for $y(t) = t^5$

Table 9 Errors for $\alpha = 0.3$ and $\alpha = 0.5$ in Example 5.4 for $y(t) = \sin t$

h	HoS (α=0.3)		M-L1 scheme ($\alpha = 0.3$)		HoS (α=0.5)		M-L1 scheme (α=0.5)	
	L_∞ error	EOC	L_∞ error	EOC	L_∞ error	EOC	L_∞ error	EOC
0.1	7.34×10^{-6}	–	7.86×10^{-5}	–	2.28×10^{-5}	–	2.13×10^{-4}	–
0.05	5.85×10^{-7}	3.64	3.88×10^{-5}	2.62	2.04×10^{-6}	3.47	3.88×10^{-5}	2.46
0.025	4.63×10^{-8}	3.66	2.03×10^{-6}	2.64	1.82×10^{-7}	3.48	6.98×10^{-6}	2.47
0.0125	3.64×10^{-9}	3.66	3.22×10^{-7}	2.65	1.62×10^{-8}	3.49	1.24×10^{-6}	2.48

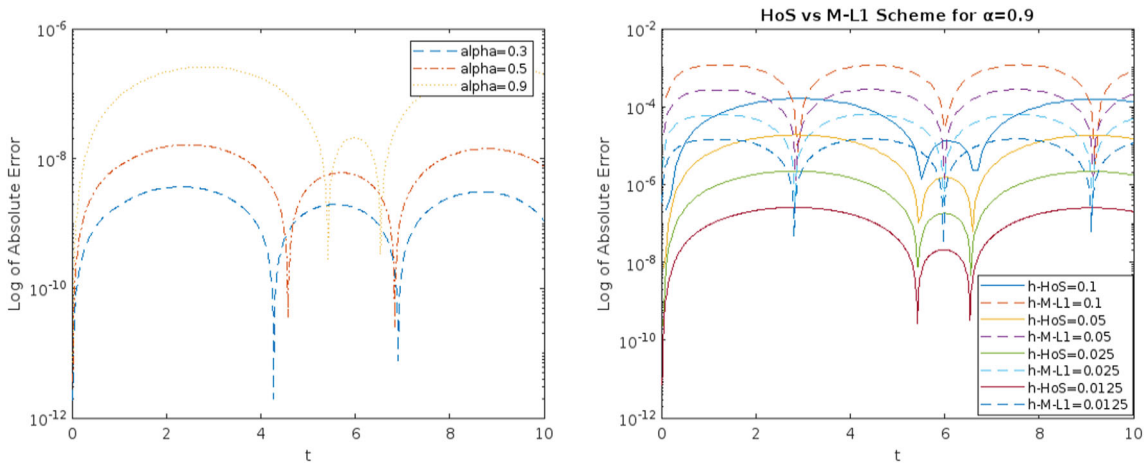

Fig. 5 Error plot of Example 5.4 for $y(t) = \sin t$

From the results in Tables 1, 2, 3, 4, 5, 6, it is evident that our scheme outperforms the M-L1 Scheme in both examples, even for the case when $i = 6$. Similar observations can be concluded for both examples from the Figs. 1a–c and 2a–c for the case $\alpha = 0.9$. Moreover, the Figs. 1d–f and 2d–f demonstrate that the errors, for $\alpha = 0.3,\ 0.5,\ 0.7$, settle down as time increases.

Example 5.3 Consider the following nonlinear FDDE

$$ {}_0^C D_t^\alpha y(t) + y(t)^3 = y(t-0.1) + g(t) \quad \text{for } t \in [0, 10], \tag{5.3} $$

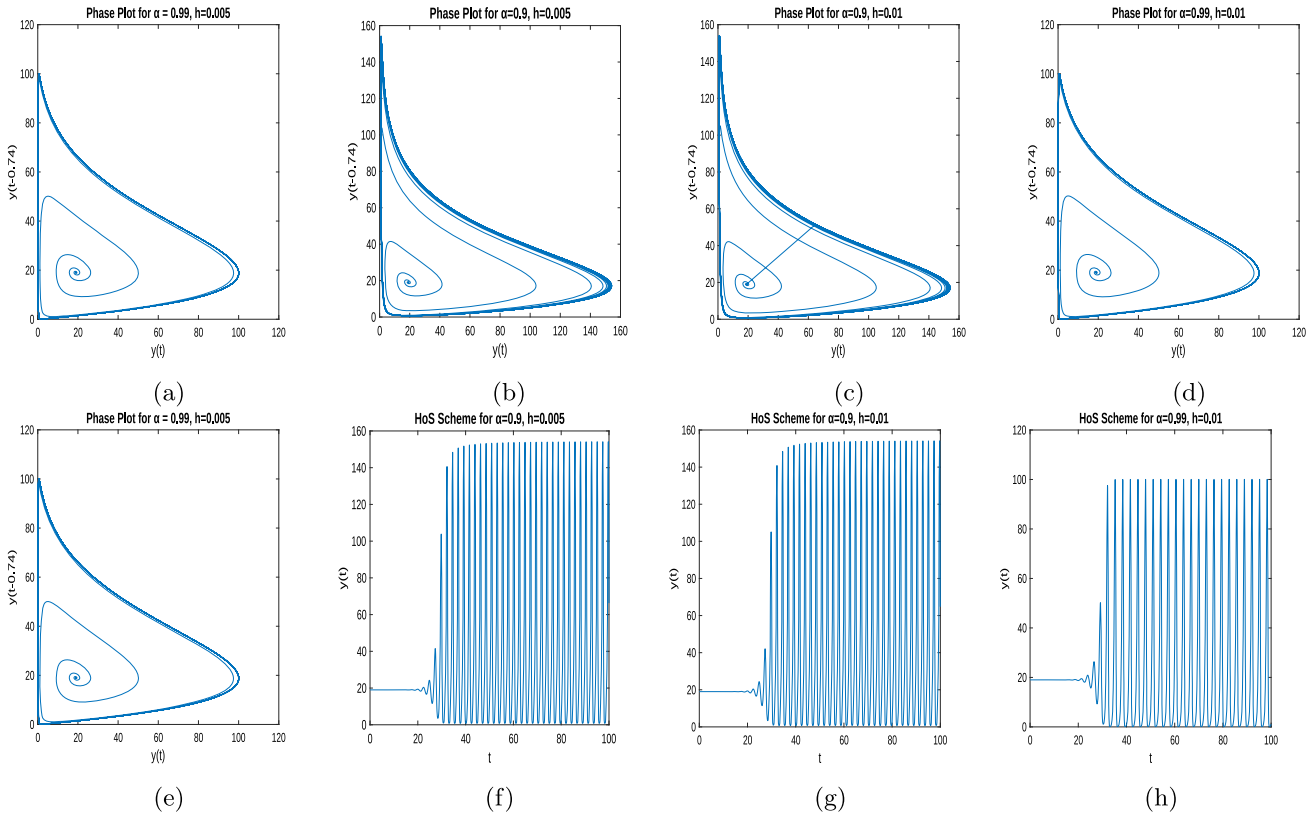

Fig. 6 Solution and phase plot of Example 5.5

Table 10 Computational time (in seconds) for *Example* 5.5.

h	α	Time(s)
0.01	0.90	31.00
	0.99	29.37
0.005	0.90	112.69
	0.99	108.88

where g be the real-valued function such that $y(t) = t^i$, $i = 4, 5$, become the exact solution of the problem (5.3) with delay function $\phi(t) = t^i$, for $i = 4, 5$, defined for $t \leq 0$, respectively.

Illustration of Example 5.3 For each $i = 4, 5$, we determined the functions g from Eq. (5.3) so that $y(t) = t^i$ become solution of (5.3). Then, for each $i = 4, 5$, we used Newton's iterative method to linearize the Eq. (5.3) and approximated the limit of the sequence of solutions of the following linear FDDEs:

$$
\begin{aligned}
{}_0^C D_t^{\alpha} y^{l+1}(t) + 3\left(y^l(t)\right)^2 y^{l+1}(t) = & y^{l+1}(t-0.1) \\
& + 2\left(y^l(t)\right)^3 + g(t) \quad \text{for } t \in [0, 10],
\end{aligned} \tag{5.4}
$$

with delay function $y^{l+1}(t) = \phi(t)$. We applied our proposed numerical scheme and compared the same with the M-L1 Scheme (Raju and Madduri 2021) for the case $\alpha = 0.9$ with different step sizes h. The obtained results are presented in Tables 7 and 8 for the cases $i = 4$ and $i = 5$, respectively. It is evident from the tables that the $L_\infty-$errors decreases with the decrease of step sizes. Further, the computational cost of our scheme is higher than the M-L1 Scheme at each step size; however, the errors obtained at each step size h are outstanding compared to those of the M-L1 Scheme. Therefore, it can also be concluded from the tables that the desired accuracy can be achieved with less time. Both the tables also establish that the EOC of the proposed HoS scheme matches with the obtained theoretical result in Theorem 4.1 with step-size $h = 0.0125$ or less. We also plotted errors obtained for both schemes and presented them in the Figs. 3 and 4.

Example 5.4 Consider the following FDDE

$$
{}_0^C D_t^{\alpha} y(t) + y(t) = y(t-1) + g(t) \quad \text{for } t \in [0, 10], \tag{5.5}
$$

where g be the real-valued function such that $y(t) = \sin t$, be the exact solution of (5.5) with the delay functions $\phi(t) = \sin t$, defined on $[-1, 0]$.

Illustration of Example 5.4 After deriving the function g, first we applied our proposed numerical scheme and M-L1 Scheme (Raju and Madduri 2021) for $\alpha = 0.3$ and $\alpha = 0.5$ with different step sizes. The obtained results are presented

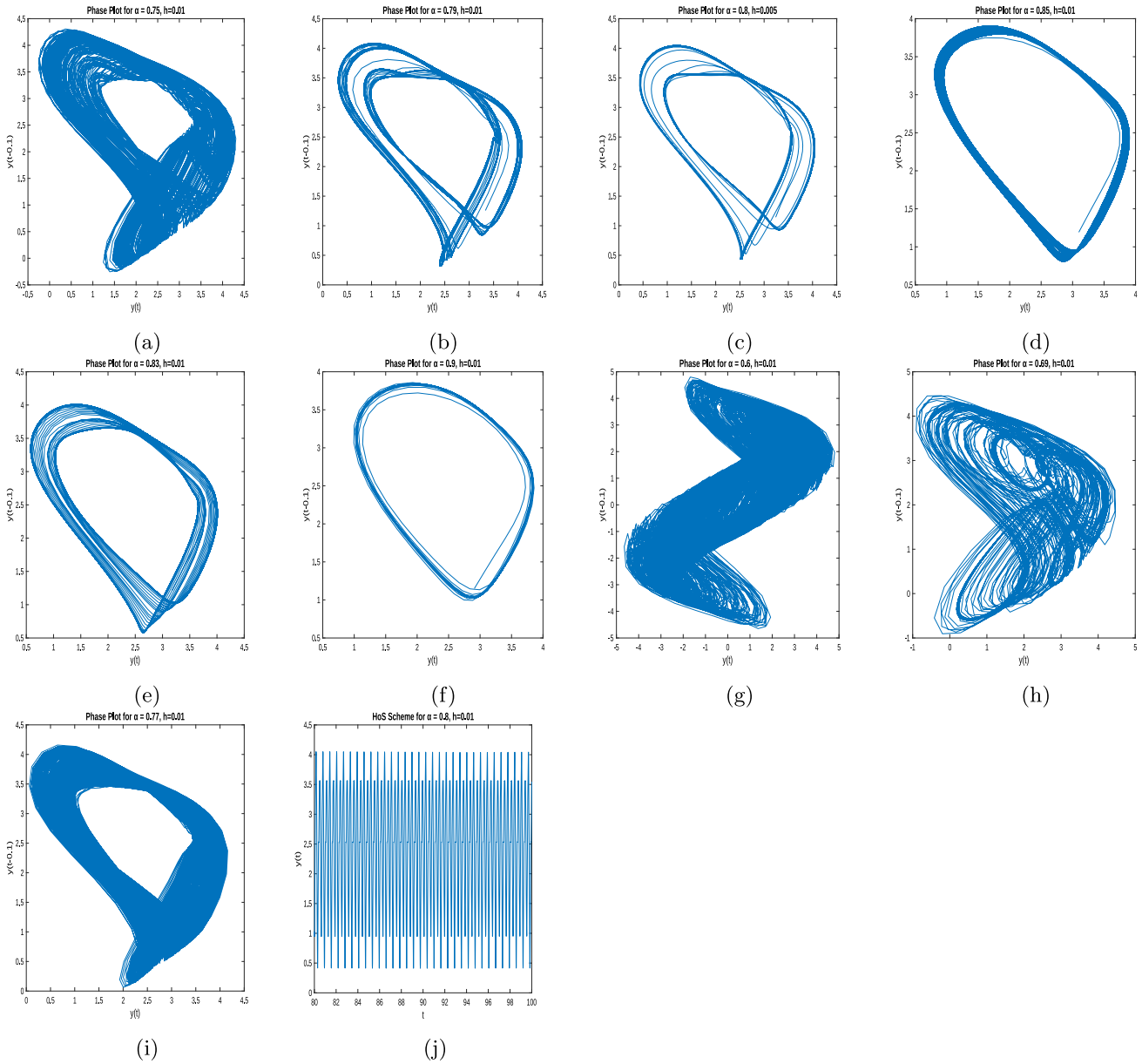

Fig. 7 Solution and phase plot of Example 5.6

Table 11 Computational time (in seconds) for *Example* 5.6 with h=0.01

α	0.6	0.69	0.7	0.8	0.75	0.77	0.79	0.83	0.85	0.9
Time(s)	32.16	31.78	33.17	32.92	32.02	31.58	32.55	32.31	31.74	31.52

in Table 9. One may observe that the proposed HoS scheme outperforms the M-L1 Scheme, $L_\infty-$error decreases with the decrease of step sizes, and the EOC matches with the derived theoretical results in the Theorem 4.1. Figure 5a shows the errors obtained in the HoS scheme versus time for different values of α with step size $h = 0.0125$. Similarly, Fig. 5b shows the errors obtained in the proposed HoS scheme and M-L1 scheme versus time for $\alpha = 0.9$ with different values of h.

Example 5.5 (Tavernini 1996) Consider the following FDDE, which represents the fractional model of a population of lemmings with a 4-year life cycle.

$$\begin{cases} {}_0^C D_t^{\alpha} y(t) = 3.5y(t)\left(1 - \dfrac{y(t-\tau)}{19}\right) & \text{for } t \in [0, 100], \\ y(t) = \phi(t) & \text{for } t \le 0, \end{cases} \tag{5.6}$$

where $\phi(0) = 19.00001,$ and $\phi(t) = 19, \quad t < 0.$

Illustration of Example 5.5: We applied our proposed numerical scheme for the cases $\alpha = 0.9,\ 0.99$ with different step sizes h, and the respective computational time (in seconds) are given in Table 10. The derived approximate solution and phase portraits from HoS are plotted in Fig. 6. One can verify that our scheme also yields similar results as given in Raju and Madduri (2021).

Example 5.6 (Bhalekar 2019) Consider the following FDDE, which is also known as the fractional Ikeda equation

$$\begin{cases} {}_0^C D_t^{\alpha} y(t) = -3y(t) + 24 \sin y(t-0.1), & \text{for } t \in [0, 100], \\ y(t) = \phi(t) = 1 & \text{for } t < 0. \end{cases} \tag{5.7}$$

Illustration of Example 5.6: We applied our proposed numerical scheme for different values of α with step size $h = 0.01$. The derived results of the approximate solution and phase diagrams based on the proposed HoS scheme are displayed in Fig. 7. The stability of the chaotic behavior of the solution can be observed from $\alpha = 0.7$. Also, the proposed HoS scheme yields similar results as given in (Raju and Madduri 2021). Further, the computational times for the proposed HoS scheme of different values of α with step size $h = 0.01$ are tabulated in Table 11.

6 Conclusion

We developed a higher-order scheme (HoS) for approximating the solutions of nonlinear FDDEs by incorporating an interpolation-based approximation of Caputo's fractional derivative. The stability results and detailed error analysis are also carried out for the proposed numerical algorithm. We investigated the performance of the proposed HoS scheme over various linear and nonlinear examples, including real-life applications. Further, we compared the derived results with the recently proposed M-L1 scheme (Raju and Madduri 2021) and noticed that the HoS scheme outperforms even with the more significant step size. We also established that the order of convergence is $4 - \alpha$, which was claimed in Theorem 4.1. In light of the LTRPS approach's high accuracy in solving fractional nonlinear equations and its easy calculation process, we intend to investigate this method further for the proposed FDDE (1.2) and design a robust numerical scheme.

Appendix

The following linearized form of Eq. (1.1) is obtained in each of Newton's iterative processes:

$$\begin{cases} {}_0^C D_t^{\alpha} y^{l+1}(t) - \left(\dfrac{\partial G}{\partial y}\right)_{(t,y^l)} y^{l+1}(t) = G(t, y^{l+1}(t-\tau), y^l(t)) - \left(\dfrac{\partial G}{\partial y}\right)_{(t,y^l)} y^l(t), \quad t \in I, \\ y^{l+1}(t) = \phi(t), \quad t \in [-\tau, 0]. \end{cases} \tag{A.1}$$

Now, the solution of the obtained sequence of FDDEs (A.1) can be approximated instead of the solution of nonlinear FDDE (1.1). The Eq.s in (A.1) can be viewed as (1.2) if we denote $y(t) = y^{l+1}(t)$, $b(t) = \left(\dfrac{\partial G}{\partial y}\right)_{(t,y^l)}$, and $g(t, y(t-\tau)) = G(t, y^{l+1}(t-\tau), y^l(t)) - \left(\dfrac{\partial G}{\partial y}\right)_{(t,y^l)} y^l(t).$

Lemma A.1 (Morgado et al. 2013; Raju and Madduri 2021) Let $y_{0\tau}(t) = \phi(t)$ for $t \in [-\tau, 0]$ and $b < 0$ on I. Also, let $k > 0$ be the greatest integer such that the function defined below is continuous:

$$\zeta_{k\tau}(t) = \begin{cases} g(t, \phi(t-\tau)) & \text{for } 0 < t \le \tau, \\ g(t, y_{\tau}(t-\tau)) & \text{for } \tau < t \le 2\tau, \\ \quad \cdot & \\ \quad \cdot & \\ \quad \cdot & \\ g(t, y_{(k-1)\tau}(t-\tau)) & \text{for } (k-1)\tau < t \le k\tau. \end{cases} \tag{A.2}$$

Then the FDDE (1.2) on the interval $[0, k\tau]$, has a solution which is given by

$$\begin{aligned} y_{l\tau}(t) &= \int_0^t (t-s)^{\alpha-1} E_{\alpha,\alpha}(b(t-s)^{\alpha}) \zeta_{l\tau}(s) ds \\ &+ p_{l\tau} E_{\alpha,1}(bt^{\alpha}), \quad \text{for } (l-1)\tau < t \le l\tau, \end{aligned} \tag{A.3}$$

where $p_{l\tau}$, $l = 1, 2, \ldots k$ is a constant and $E_{\alpha,\beta}$ denotes the Mittag–Leffler function defined by

$$E_{\alpha,\beta} = \sum_{k=0}^{\infty} \frac{z^k}{\Gamma(\alpha k + \beta)}, \ z, \beta \in \mathbb{C}, \ Re(\alpha) > 0.$$

Lemma A.2 The constants c_r, m_r, n_r defined in the Eq. (2.5) will satisfy the following:

$$n_r + m_{r-1} - 2n_{r-1} + c_{r-2} - m_{r-2} + n_{r-2} > 0, \quad \forall\ r \geq 3. \tag{A.4}$$

Proof For $r \geq 3$, it is easy to derive the following equality:

$$\begin{aligned}
&n_r + m_{r-1} - 2n_{r-1} + c_{r-2} - m_{r-2} + n_{r-2} \\
&= \frac{h^{-\alpha}}{\Gamma(1-\alpha)}\Bigg\{\Bigg(\frac{d_r^{3-\alpha}}{2} - (r+2)d_r^{2-\alpha} \\
&\quad + \frac{d_r^{1-\alpha}}{6}(2(r+2)^2 + (r+3)(r+1)\Bigg) \\
&\quad + \left(\left(r+\frac{3}{2}\right)d_{r-1}^{1-\alpha} - d_{r-1}^{2-\alpha}\right) \\
&\quad - \Bigg(d_{r-1}^{3-\alpha} - 2(r+1)d_{r-1}^{2-\alpha} + \frac{d_{r-1}^{1-\alpha}}{3}(2(r+1)^2 \\
&\quad + r(r+2))\Bigg) + d_{r-2}^{1-\alpha} - \left(\left(r+\frac{1}{2}\right)d_{r-2}^{1-\alpha} - d_{r-2}^{2-\alpha}\right) \\
&\quad + \left(\frac{d_{r-2}^{3-\alpha}}{2} - rd_{r-2}^{2-\alpha} + \frac{d_{r-2}^{1-\alpha}}{6}(2r^2 + (r+1)(r-1))\right)\Bigg\} \\
&= \frac{h^{-\alpha}}{\Gamma(1-\alpha)}\Big[\theta(r) - \theta(r-1)\Big],
\end{aligned}$$

where the function θ is defined as

$$\begin{aligned}
\theta(s) =& \frac{(s+1)^{3-\alpha} - 2s^{3-\alpha} + (s-1)^{3-\alpha}}{(1-\alpha)(2-\alpha)(3-\alpha)} \\
&+ \frac{(s-1)^{2-\alpha} - 2s^{2-\alpha} + (s+1)^{2-\alpha}}{(1-\alpha)(2-\alpha)} \\
&+ \frac{(s-1)^{1-\alpha} - 2s^{1-\alpha} + (s+1)^{1-\alpha}}{3(1-\alpha)}.
\end{aligned}$$

On differentiating the function θ, we get

$$\theta'(s) = \delta(s) - \delta(s-1),$$

where the function δ will be given by

$$\begin{aligned}
\delta(s) =& \frac{(s+1)^{2-\alpha} - s^{2-\alpha}}{(1-\alpha)(2-\alpha)} \\
&+ \frac{(s+1)^{1-\alpha} - s^{1-\alpha}}{(1-\alpha)} \\
&+ \frac{(s+1)^{-\alpha} - s^{-\alpha}}{3}.
\end{aligned}$$

Now, on differentiating the function δ, we get

$$\delta'(s) = \eta(s) - \eta(s-1).$$

Here, the function η is given by

$$\eta(s) = \frac{(s+1)^{1-\alpha}}{1-\alpha} + (s+1)^{-\alpha} - \frac{\alpha}{3}(s+1)^{-1-\alpha}$$

and its derivative will be

$$\eta'(s) = \left[(s+1)(s+1-\alpha) + \frac{\alpha(\alpha+1)}{3}\right](s+1)^{-\alpha-2}.$$

It is easy to see that $\eta'(s) \geq 0$ for each $s \geq 3$. Therefore, the function η is increasing, and so are the functions δ and θ for $r \geq 3$. This establishes our claim. □

Lemma A.3 There exists a constant $M > 0$ such that the truncation error R_2, defined in (2.5), satisfies

$$|\, R_2 \,| \leq Mh^{4-\alpha}.$$

Furthermore, the following holds true

$$|\zeta_{k\tau}(t_r) - \zeta_{k\tau}^r| \leq \begin{cases} 0 & \text{for } 0 < t_r \leq \tau, \\ \frac{7}{2}Mh^{4-\alpha} & \text{for } \tau < t_r \leq 2\tau, \\ \sum_{i=1}^{2}\left(\frac{7}{2}\right)^i Mh^{4-\alpha} & \text{for } 2\tau < t_r \leq 3\tau, \\ \vdots & \\ \sum_{i=1}^{r-1}\left(\frac{7}{2}\right)^i Mh^{4-\alpha} & \text{for } (k-1)\tau < t_r \leq k\tau. \end{cases} \tag{A.5}$$

Proof From the Eq.s (2.3) and (2.5), one may derive the following explicit expression for R_2:

$$R_2 = \frac{1}{\Gamma(1-\alpha)}\sum_{j=1}^{r}\int_{t_{j-1}}^{t_j}(t_r - s)^{-\alpha}R_{1,j}'(s)ds,$$

where

$$\begin{aligned}
R_{1,j}'(t) =& \frac{y^{(4)}(\xi_j)}{4!}\Big\{(t-t_j)(t-t_{j-1})(t-t_{j-2}) + (t-t_j)(t-t_{j-1})(t-t_{j-3}) \\
&+ (t-t_j)(t-t_{j-2})(t-t_{j-3}) + (t-t_{j-1})(t-t_{j-2})(t-t_{j-3})\Big\}.
\end{aligned}$$

Now, from (Li et al. 2016), we get:

$$|R_2| \leq C_1\left[\max_{0\leq\zeta\leq T} y^{(4)}(\zeta)\right]h^{4-\alpha} = Mh^{4-\alpha}.$$

For $t_r \in [0, \tau]$, we have $\zeta_{k\tau}(t_r) = \zeta_{k\tau}^r$. Hence,

$$|\zeta_{k\tau}(t_r) - \zeta_{k\tau}^r| = 0.$$

The definitions of y_r and $y(t_r)$ in the Eqs. (2.6)–(2.8) and (2.9)–(2.11) along with the obtained result imply that

$$| y_r - y(t_r) | = | R_2 | \leq \frac{7}{2} M h^{4-\alpha} \text{ for } t_r \in [0, \tau]. \tag{A.6}$$

Next, we consider the case $t_r \in [0, 2\tau]$. From the definition of the function $\zeta_{k\tau}$ in (A.2) and the function $\zeta_{k\tau}^r$ in the equations (2.9)-(2.11), we have

$$|\zeta_{k\tau}(t_r) - \zeta_{k\tau}^r| = \begin{cases} 0 & \text{for } 0 < t_r \leq \tau, \\ |g(t_r, y_\tau(t_r - \tau)) - g(t_r, y_1^{r-\tau})| & \text{for } \tau < t_r \leq 2\tau, \end{cases} \tag{A.7}$$

where $y_1^{r-\tau}$ represents the approximate value of $y_\tau(t_r - \tau)$ using the designed scheme (2.9)–(2.11) over the interval $[\tau, 2\tau]$. Therefore, we have

$$|\zeta_{k\tau}(t_r) - \zeta_{k\tau}^r| \leq \begin{cases} 0 & \text{for } 0 < t_r \leq \tau, \\ \frac{7}{2} M h^{4-\alpha} & \text{for } \tau < t_r \leq 2\tau. \end{cases}$$

Using the above inequality, and the Eqs. (2.6)–(2.8) and (2.9)–(2.11), one can derive the following

$$|y_r - y(t_r)| \leq \begin{cases} \frac{7}{2} M h^{4-\alpha} & \text{for } 0 < t_r \leq \tau, \\ \sum_{i=1}^{2} \left(\frac{7}{2}\right)^i M h^{4-\alpha} & \text{for } \tau < t_r \leq 2\tau. \end{cases}$$

Assume that the inequality (A.5) holds true for any $t_r \in [0, (k-1)\tau]$. Then, the Eqs. (2.6)–(2.8) and (2.9)–(2.11) imply the following result:

$$|y_r - y(t_r)| \leq \begin{cases} \frac{7}{2} M h^{4-\alpha} & \text{for } 0 < t_r \leq \tau, \\ \sum_{i=1}^{2} \left(\frac{7}{2}\right)^i M h^{4-\alpha} & \text{for } \tau < t_r \leq 2\tau, \\ \sum_{i=1}^{3} \left(\frac{7}{2}\right)^i M h^{4-\alpha} & \text{for } 2\tau < t_r \leq 3\tau, \\ \cdot & \\ \cdot & \\ \cdot & \\ \sum_{i=1}^{k-1} \left(\frac{7}{2}\right)^i M h^{4-\alpha} & \text{for } (k-2)\tau < t_r \leq (k-1)\tau. \end{cases} \tag{A.8}$$

Next, we establish the result for the case $t_r \in [0, k\tau]$. Now, the definitions of the functions $\zeta_{k\tau}$ and $\zeta_{k\tau}^r$ in the Eqs. (A.2) and (2.9)–(2.11), respectively, imply that

$$|\zeta_{k\tau}(t_r) - \zeta_{k\tau}^r| = \begin{cases} 0 & \text{for } 0 < t_r \leq \tau, \\ |g(t_r, y_\tau(t_r - \tau)) - g(t_r, y_1^{r-\tau})| & \text{for } \tau < t_r \leq 2\tau, \\ |g(t_r, y_{2\tau}(t_r - \tau)) - g(t_r, y_2^{r-\tau})| & \text{for } 2\tau < t_r \leq 3\tau, \\ \cdot & \\ \cdot & \\ \cdot & \\ |g(t_r, y_{(k-1)\tau}(t_r - \tau)) - g(t_r, y_{(k-1)}^{r-\tau})| & \text{for } (k-1)\tau < t_r \leq k\tau, \end{cases} \tag{A.9}$$

where $y_l^{r-\tau}$ denotes the approximate value of $y_{l\tau}(t_r - \tau)$, for $l = 1, 2, ..., k-1$, using the designed scheme (2.9)–(2.11). Now, using the inequality (A.8), the claim in (A.5) holds. □

Funding No funds, grants or support received for the submitted work.

Declarations

Conflict of interest On behalf of all authors, the corresponding author states that there is no conflict of interest.

References

Admon MR, Senu N, Ahmadian A, Majid ZA, Salahshour S (2023) A new efficient algorithm based on feedforward neural network for solving differential equations of fractional order. Commun Nonlinear Sci Numer Simul 117:106968

Agarwal P, Choi J (2016) Fractional calculus operators and their image formulas. J Korean Math Soc 53(5):1183–1210

Agarwal P, Sunarto A, Chew JVL, Sulaiman J, Momani S (2023) New preconditioning and half-sweep accelerated overrelaxation solution for fractional differential equation. J King Saud Univ-Sci 35(2):102461

Agiza HN, Sohaly MA, Elfouly MA (2023) Small two-delay differential equations for Parkinson's disease models using Taylor series transform. Indian J Phys 97(1):39–46

Alshammari S, Alshammari M, Alabedalhadi M, AlSawalha MM, Al-Smadi M (2024) Numerical investigation of a fractional model of a tumor-immune surveillance via Caputo operator. Alex Eng J 86:525–536

Atangana A, Secer A (2013) A note on fractional order derivatives and table of fractional derivatives of some special functions. Abstr Appl Anal 2013:279681

Atangana A (2018) Fractional operators and their applications. In: Atangana A (ed) Fractional operators with constant and variable order with application to geo-hydrology. Academic Press, Cambridge, pp 79–112

Behera S, Ray SS (2022) An efficient numerical method based on Euler wavelets for solving fractional order pantograph Volterra delay-integro-differential equations. J Comput Appl Math 406:113825

Bhalekar S (2019) Analysing the stability of a delay differential equation involving two delays. Pramana 93:1–7

Chen Y, Liu F, Yu Q, Li T (2021) Review of fractional epidemic models. Appl Math Model 97:281–307

Delavari H, Jokar R (2021) Intelligent fractional-order active fault-tolerant sliding mode controller for a knee joint orthosis. J Intell Robot Syst 102(2):39

Deng W, Li C, Lü J (2007) Stability analysis of linear fractional differential system with multiple time delays. Nonlinear Dyn 48:409–416

Diethelm K, Ford N J (2010) The analysis of fractional differential equations. Lecture notes in mathematics 2004

Dubey S, Sharma M (2014) Solutions to fractional functional differential equations with nonlocal conditions. Fract Calc Appl Anal 17(3):654–673

Elango S (2023) Second-order singularly perturbed delay differential equations with non-local boundary condition. J Comput Appl Math 417:114498

Faheem M, Khan A, Wong PJ (2022) A Legendre wavelet collocation method for 1D and 2D coupled time-fractional nonlinear diffusion system. Comput Math Appl 128:214–238

Haque I, Ali J, Mursaleen M (2023) Solvability of an infinite system of Langevin fractional differential equations in a new tempered sequence space. Fract Calc Appl Anal 26(4):1894–1915

Jhinga A, Daftardar-Gejji V (2019) A new numerical method for solving fractional delay differential equations. Comput Appl Math 38:1–18

Jumarie G (2009) Table of some basic fractional calculus formulae derived from a modified Riemann-Liouville derivative for non-differentiable functions. Appl Math Lett 22(3):378–385

Khirsariya SR, Chauhan JP, Rao SB (2024) A robust computational analysis of residual power series involving general transform to solve fractional differential equations. Math Comput Simul 216:168–186

Krol K (2011) Asymptotic properties of fractional delay differential equations. Appl Math Comput 218(5):1515–1532

Kürkçü ÖK, Aslan E, Sezer M (2019) An integrated numerical method with error analysis for solving fractional differential equations of quintic nonlinear type arising in applied sciences. Math Methods Appl Sci 42(18):6114–6130

Lakshmikantham V (2008) Theory of fractional functional differential equations. Nonlinear Anal: Theory, Methods Appl 69(10):3337–3343

Lazarević MP, Spasić AM (2009) Finite-time stability analysis of fractional order time-delay systems: Gronwall's approach. Math Comput Model 49(3–4):475–481

Li H, Cao J, Li C (2016) High-order approximation to Caputo derivatives and Caputo-type advection-diffusion equations (III). J Comput Appl Math 299:159–175

Liao C, Ye H (2009) Existence of positive solutions of nonlinear fractional delay differential equations. Positivity 13:601–609

Maes F, Van BK (2023) Existence and uniqueness of a weak solution to fractional single-phase-lag heat equation. Fract Calc Appl Anal 26(4):1663–1690

Belhamiti MM, Dahmani Z, Agarwal P (2022) Chaotic Jerk circuit: Existence and stability of solutions for a fractional model. Prog Fract Differ Appl 9(3):409–419

Morgado M, Ford N, Lima P (2013) Analysis and numerical methods for fractional differential equations with delay. J Comput Appl Math 252:159–168

Pituk M, Stavroulakis IP, Stavroulakis JI (2023) Explicit values of the oscillation bounds for linear delay differential equations with monotone argument. Commun Contemp Math 25(03):2150087

Rahimkhani P, Ordokhani Y (2019) A numerical scheme based on Bernoulli wavelets and collocation method for solving fractional partial differential equations with Dirichlet boundary conditions. Numer Methods Partial Differ Equ 35(1):34–59

Raju G, Madduri H (2021) Higher order numerical schemes for the solution of fractional delay differential equations. J Comput Appl Math 402:113810

Rehman A, Singh R, Agarwal P (2022) On fractional Lyapunov functions of nonlinear dynamic systems and Mittag-Leffler stability thereof. Foundations 2(1):209–217

Rivero M, Trujillo JJ, Vázquez L, Pilar VM (2011) Fractional dynamics of populations. Appl Math Comput 218(3):1089–1095

Sabir A, Rehman M (2023) A numerical method based on quadrature rules for ψ-fractional differential equations. J Comput Appl Math 419:114684

Salahshour S, Ahmadian A, Senu N, Baleanu D, Agarwal P (2015) On analytical solutions of the fractional differential equation with uncertainty: Application to the basset problem. Entropy 17:885–902

Sandoz A, Ducret V, Gottwald GA, Vilmart G, Perron K (2023) SINDy for delay-differential equations: application to model bacterial zinc response. Proc R Soc A 479(2269):20220556

Sene N (2022) Second-grade fluid with Newtonian heating under Caputo fractional derivative: analytical investigations via laplace transforms. Math Modell Numer Simul Appl 2(1):13–25

Samko SG, Kilbas AA, Marichev OI (1993) Fractional integrals and derivatives: theory and applications. Gordon and Breach Science, Switzerland

Sharma M (2021) Solvability and optimal control of nonautonomous fractional dynamical systems of neutral-type with nonlocal conditions. Iran J Sci Technol, Trans A: Sci 45:2121–2133

Sharma M (2023) Existence of optimal pairs and solvability of non-autonomous fractional sobolev-type integrodifferential equations. Indian J Pure Appl Math 1:12

Sharma M, Dubey S (2017) Analysis of fractional functional differential equations of neutral type with nonlocal conditions. Diff Equ Dyn Syst 25:499–517

Sriwastav N, Barnwal AK, Wazwaz AM, Singh M (2023) A novel numerical approach and stability analysis for a class of pantograph delay differential equation. J Comput Sci 67:101976

Tavernini L (1996) Continuous-time modeling and simulation: using Turbo Pascal and CTMS/TP. Gordon and Breach Science Publishers Inc., United States

Yan Y, Khan M, Ford N (2018) An analysis of the modified l1 scheme for time-fractional partial differential equations with nonsmooth data. SIAM J Numer Anal 56:210–227

Yang Z, Li Q, Yao Z (2023) A stability analysis for multi-term fractional delay differential equations with higher order. Chaos, Solitons & Fractals 167:112997

Zaky M, Van BK, Taha T, Suragan D, Hendy A (2023) An l1 type difference/galerkin spectral scheme for variable-order time-fractional nonlinear diffusion-reaction equations with fixed delay. J Comput Appl Math 420:114832

Zaky MA, Hendy AS, Macías-Díaz JE (2020) Semi-implicit Galerkin-Legendre spectral schemes for nonlinear time-space fractional diffusion-reaction equations with smooth and nonsmooth solutions. J Sci Comput 82:1–27